BEST AVAILABLE IMAGES

Defective images within this document are accurate representations of the original documents submitted by the applicant.

Defects in the images may include (but are not limited to):

- BLACK BORDERS
- TEXT CUT OFF AT TOP, BOTTOM OR SIDES
- FADED TEXT
- ILLEGIBLE TEXT
- SKEWED/SLANTED IMAGES
- COLORED PHOTOS
- BLACK OR VERY BLACK AND WHITE DARK PHOTOS
- GRAY SCALE DOCUMENTS

IMAGES ARE BEST AVAILABLE COPY.

As rescanning documents *will not* correct images, please do not report the images to the Image Problem Mailbox.

COMPLETE LISTING OF ALL CLAIMS IN THE APPLICATION

1-28 (canceled)

29. (previously presented) A method for treating migrainous cerebrovascular disorders which comprises administering to a subject in need thereof an effective amount of at least one binding partner for a 5-HT5-receptor whose binding affinity for the 5-HT5-receptor is at least 10 times greater than its binding affinity for a 5-HT1D-receptor.

30. (previously presented) The method as claimed in claim 29, where the binding affinity of the binding partner for a 5-HT5-receptor is at least 20 times greater than its binding affinity for a 5-HT1D-receptor.

31. (previously presented) The method as claimed in claim 29, where the binding affinity of the binding partner for a 5-HT5-receptor is at least 50 times greater than its binding affinity for a 5-HT1D-receptor.

32. (previously presented) The method as claimed in claim 29, where the K_i value for binding of the binding partner to the 5-HT5-receptor is less than 10^{-8} M.

33. (canceled)

34. (previously presented) The method as claimed in claim 29, wherein the migrainous cerebrovascular disorder is migraine.

35. (previously presented) The method as claimed in claim 34, wherein the binding partner is administered when acute symptoms of migraine occur.

36. (previously presented) The method as claimed in claim 34, wherein the migraine is

a disorder selected from the group consisting of associated migraine, migraine equivalents, digestive migraine, ophthalmic migraine, ophthalmoplegic migraine, migraine rouge, cluster headache and cervical migraine.

37. (new) The method as claimed in claim 34, wherein the binding partner is active in at least one animal model for migraine.

38. (new) The method as claimed in claim 37, wherein the animal model is selected from the group consisting of models which are based on protein extravasation induced by stimulation of trigeminal ganglia, distribution of the carotide blood flow, nitroglycerin-induced c-fos gene expression and translocation, retinal spreading depression, or cortical spreading depression.

8 Cortical spreading depression and migraine

Simon J Read, Andrew A Parsons

INTRODUCTION

Cortical spreading depression (CSD) was originally described by Leao[1] as a slowly spreading depression of electroencephalographic activity in the rabbit neocortex. CSD produces a range of neurophysiological vascular and metabolic disturbances linking metabolic activity with long-term changes in trigeminovascular activity. This link between the numerous systems involved in vessel activity and sensory perception provides a potentially attractive role for CSD as a generator of central sensitization and cortical hyperexcitability in migraine. This review is a critical appraisal of current knowledge of the integrating role of CSD in migraine.

THE PHENOMENON OF CSD

Cortical spreading depression is characterized as a transient disturbance in mechanisms maintaining ionic homeostasis which propagates across the cortex at a defined velocity of 2–5 mm min^{-1}.[2] During the propagation of CSD, the local extracellular ionic environment acidifies and accumulates K^+ (60–80 mM) whilst Na^+ and Cl^- redistribute to intracellular compartments.[3] In the non-ischaemic intact cortex, re-establishment of membrane potential is an energy-dependent phenomena and therefore a functional hyperaemia provides increased nutrient input adequate for metabolic demand. This complex interaction between neuronal and glial energy metabolism and the vascular compartment is mediated by local changes in the interstitial microenvironment, including lowered pH and neurotransmitter release.

ANIMAL MODELS

The experimental phenomenon of CSD has been extensively studied in animal models and therefore it is important to note that the selection of an appropriate animal model of CSD is dependent on the pathophysiological and pharmacological relevance to humans. It is apparent that in experimental animals, induction of CSD in higher species may occur with greater difficulty. These observations may be a reflection of an increase in ratio of glial/non-glial cells, and hence extracellular buffering capacity, in higher species.[3] Similarly, propagation of CSD also appears to be limited with increasing complexity of cortical architecture. As reviewed by Gardiner-Medwin,[4] this propagation failure has been observed in humans and nonhuman primates.[5]

In the gyrencephalic cat brain, repeated waves

of CSD can be induced following application of a chemical stimulus. In this model, the onset of a prolonged cortical instability evokes reproducible changes in pial artery diameter, bloodflow and neurotransmitter release, independent of an ischaemic insult.[5–7]

The resistance of higher species to propagation of CSD may offer a partial explanation of the limited observations of CSD-like phenomena in humans. Other complicating factors may include the role of different anaesthetic regimes. Piper and Lambert[8] have demonstrated an inhibitory effect of cortical anaesthetics on spreading depression in cats. Isoflurane and particularly halothane, both commonly used clinical anaesthetics, inhibit the genesis of CSD and therefore have important implications for observations in humans.

These considerations should be taken into account in terms of modelling CSD in experimental animals. Key differences in the frequency of cortical depolarization, ratios of glial/neuronal cells, anaesthetic regimes and differences in release of neurotransmitters and metabolic coupling require consideration. Therefore, although the use of species such as the rat may provide a useful model of many aspects of CSD, it may not allow investigation of numerous potential inhibitory mechanisms present in higher species. Repetitive CSD activity can be induced in the complex brain and it is clear that similarities do exist between cats and nonhuman primates, so comparisons between gyrencephalic species are valid.

METABOLIC AND VASCULAR PERTURBATIONS DURING CSD

Metabolic changes during CSD

Restoration of the extracellular and intracellular ionic milieu post-CSD is an energy-dependent process.[9–11] Initial studies of cortical glucose use during the passage of a wave of spreading depression by Shinohara et al[9] and Gjedde et al[12] indicate that a marked increase in glucose use occurs along with an increase in net transfer of glucose from blood to brain. These changes in glucose metabolism were found to occur in advance of changes in ionic milieu or regional cerebral bloodflow. Subsequent studies by Mraovitch et al[13] examining local cortical glucose use after CSD have shown that while glucose use normalizes to contralateral hemisphere levels, subcortical glucose use, particularly in the upper and lower brainstem, remains altered. Therefore, it is apparent that while CSD induces marked alterations in glucose metabolism in the cortex, it also induces prolonged changes in metabolism of subcortical structures which exceeds the time course of the initial cortical event. Mraovitch et al[13] suggested that as such, this observation may represent a suitable site for integration of the cortical phenomenon of spreading depression with other symptomatology concurrent in migraine.

Concomitant with increases in glucose metabolism, labile phosphate turnover (AMP, ADP, ATP and phosphocreatine) is also augmented during CSD. Mies and Paschen[14] have reported a 12% depression in tissue ATP content preceding the negative cortical direct current (DC) deflection, increasing to a maximum reduction of 54% at peak DC deflection. A subsequent return to normal ATP concentration on restoration of DC potential was also recorded. Lauritzen et al[15] further examined the energy status of the cortex following single CSD depolarizations in the rat. The net energy charge[16] during CSD remained buffered, although the turnover rates of ATP catabolic and anabolic pathways were increased, which was reflected by decreased levels of tissue glucose and glycogen and increased lactate. These apparent differences may be a consequence of differing experimental protocol, in particular temporal resolution and sensitivity of ATP measurements. However collectively, these data demonstrate that phosphate metabolic pathways are activated following CSD.

Changes in energy metabolism have also been noted in migraine patients with and without aura using magnetic resonance spectroscopy. Barbiroli et al[17] studied patients between attacks and noted decreased cortical phosphocreatine levels, increased ATP catabolism and lowered phosphorylation potential. Similarly, Welch et al[18] in a study encompassing 12 migraineurs with and without aura, documented decreased phosphocreatine and increased inorganic phosphate levels in the cerebral cortex between attacks in nine patients. Migraine is therefore associated with an increased metabolic demand or consumption of energy which is consistent with a neurogenic locus for the precipitation of a migraine attack.

Despite these major alterations in metabolic demand, spreading depression does not appear to be 'neurodestructive' in the nonischaemic cortex. Intracellular calcium concentrations only increase to a fraction of the levels found in the ischaemic brain and are probably buffered effectively within the cell.[19] However, alterations in energy balance, such as profound hypoglycaemia, may exacerbate the effects of raised intracellular calcium concentrations and reveal a neurodegenerative effect of CSD.[20]

Vascular changes during CSD

CSD and changes in regional cerebral blood flux

Changes in cerebral bloodflow in animal models of spreading depression have been well documented. Early studies of Leao,[1] identified changes in the vascular compartment during the spreading wave of EEG suppression. With the advent of more recent techniques to quantify changes in bloodflow the effects of spreading depression on changes in cerebral bloodflow have been investigated in detail. Long-lasting decreases in cerebral bloodflow have been identified in the cortex of anaesthetized animals.[21–24] In these models, it is important to note that although flow was decreased following spreading depression, cerebral bloodflow is maintained above critical threshold values for ischaemia. Similar spreading oligaemia has been noted in migraine with aura patients when headache was induced by carotid angiography procedures. Numerous studies have investigated the temporal aspects of decreases in flow during the migraine attack. Early studies have been extensively reviewed by Olesen.[25] A number of methodological questions have been posed surrounding ^{133}Xe clearance techniques which were available during the 1980s. However, more recent data strongly support the early concept of a spreading oligaemia occurring during migraine. Regional cerebral bloodflow assessed during a spontaneous migraine attack demonstrated a bilateral spreading oligaemia of the cortex propagating at a rate consistent with cortical spreading depression.[26] Similarly, studies in red-wine-induced headache have also confirmed spreading oligaemia originating from the visual cortex with additional changes in flow consistent with activation of nociceptive pathways.[27] Evidence for a migraine 'generator' region has also been proposed following a PET

study in spontaneous migraine,[27] increases in cortical bloodflow and regions of the thalamus were observed during migraine and treatment of this attack with sumatriptan normalized regional cerebral bloodflow changes in the cortex but had no effect on the changes in bloodflow in the brainstem.[28] These studies have been taken to demonstrate the presence of a 'generator' region for migraine and provide evidence for the symptomatic effects of polytriptan therapy.

However, a number of issues need to be considered when interpreting regional cerebral bloodflow changes in migraine. Local bloodflow will increase in regions where metabolic demand is increased. During a spontaneous or provoked migraine attack, the net response will depend on the integration of pathways activated during the migraine process and pathways activated because of the migraine process. Pain, nausea, anxiety and 'emotional well-being' may all provide activation of specific CNS areas, which complicates interpretation of data.

Collectively, recent evidence supports the concept of a spreading oligaemia occurring in migraine patients, which is consistent with the effects of spreading depression in experimental models. Magnetic resonance imaging (MRI) of rats during CSD by Gardner-Medwin et al[29] using a T_1-/gradient echo protocol showed increases of 15% in signal intensity during the passage of a CSD wave. This increase in signal intensity could be attributed to increased tissue bloodflow and concomitant decrease in oxygen coefficient of extraction. Elegant studies of Cao et al[30] which used functional MRI with blood oxygen level dependent contrast (BOLD) imaging to study occipital cortex function during visually evoked headache in migraine patients, detected a spreading neurovascular event consistent with CSD. In both migraine with and without aura subjects, estimated BOLD suppression occurred before the onset of headache and spread over the cortex at a rate between 3–6 mm min^{-1}. No alteration in BOLD effect was seen in 'normal' patients. The authors concluded that the signal change was probably due to a primary neuronal event and followed by a secondary regional cerebral bloodflow change.

CSD and changes in the pial circulation

In animal models the CSD-induced cerebral bloodflow response consists of an initial transient increase in flow followed by a long-lasting decrease.[2,29,30] However, components of CSD-induced vasomotion do vary between species as varying degrees of pial artery vasodilatation are noted in various animal species both during and immediately after cortical depolarization (Table 8.1).

Local neurotransmitter release has been implicated as a mechanism of the CSD-induced transient vasodilatation. Neurotransmitter release may occur from perivascular axons, glia and parenchyma in the dynamic coupling of arterial reactivity to CSD neuronal activation. The relative contribution of these chemical mediators also varies with species and cortical territory. For example, experiments by Wahl et al[31] in rats, using subarachnoid application of the nitric oxide synthase inhibitor, N^G nitro-L-arginine and the calcitonin gene-related peptide receptor antagonist, $CGRP_{8-37}$, demonstrated that CSD-induced vasodilatation was reduced by 50% following application of N^G nitro-L-arginine (10^{-4} M) or $CGRP_{8-37}$ (10^{-7} M) and by 75% following co-administration. In rats, although, there may be a CGRP component to CSD-induced vasodilatation, it has been suggested to be of less importance in comparison to N^G nitro-L-arginine-sensitive dilatation.[31]

Previous studies of nitric oxide release during CSD have been limited to either indirect assay of nitric oxide synthase (NOS) activity, for example measurement of citrulline[32,33] or the use of non-specific NOS inhibitors.[34,35] These techniques provide either a temporal and spatial average of total NO release during CSD. We have assessed local, moment-to-moment concentrations of cortical NO during CSD using an NO-sensitive electrode. Following CSD induction, a multiphasic NO release occurs, with the peak amplitude similar in magnitude to that recorded in cerebral ischaemia studies (Figure 8.1).[5,29] In our studies in rats, this release of NO was often not directly related to a change in region cerebral blood flux and may represent an additional effect of NO such as stimulation of nociceptive afferents.[37]

In migraine patients NO has been shown to produce migraine headache.[38] Intravenous administration of the NO donor, glyceryl trinitrate (GTN) into patients with no history of migraine and into migraineurs induces a dose-dependent and immediate headache for the duration of the infusion.[39] In migraine sufferers, this

Table 8.1 Differential degrees of vasodilatation between species during and post CSD (percentage of baseline)[41]

Species	Maximum dilatation during CSD (%)	Post CSD
Cat	ca 40	Return to baseline
Cat	ca 28	Prolonged dilatation
Rabbit	50	Return to baseline
Rabbit	57–71	Return to baseline
Rat	84	Constriction

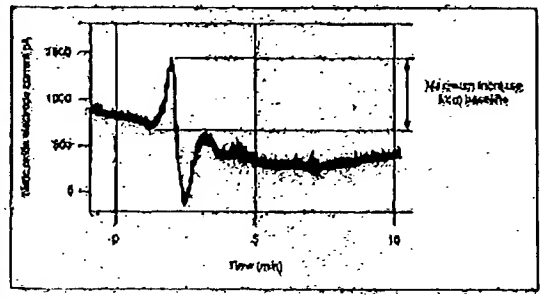

Fig. 8.1 Multiphasic release of nitric oxide.

immediate GTN headache is followed by a delayed migraine attack approximately 1 to several hours after termination of GTN infusion.[38,40] We have shown that administration of GTN in a cat model of CSD induces an immediate elevation in cortical nitric oxide release followed by a potentiation of CSD-induced release of NO with no effect on CSD-induced laser Doppler flux or pial artery diameter increases.[41] Collectively these results show nitric oxide contributes to CSD-induced vasodilatation, however, other mediators such as CGRP and local pH may also be involved. Resting cerebral bloodflow may also alter the individual contribution and role of neurotransmitters in functional coupling of flow and metabolism in CSD. Systemic administration of NOS inhibitors produces a decrease in regional cerebral blood flux and completely blocks CSD-induced vasodilatation and NO release.[51] Local, subarachnoid administration of NOS inhibitors attenuates but does not completely block CSD-induced effects and has no effect on resting arterial diameter.[51]

CSD and changes in vascular reactivity and autoregulation

Changes in resting cerebral bloodflow may therefore have important consequences on the effects of CSD. However, CSD has been reported to produce profound effects on autoregulation of cerebral bloodflow. Marked loss of reactivity to local acidification and alkalinization have been documented in cats and rats following CSD. Additionally, using iodoantipyrine autoradiographic assessment of cerebral flow, loss of autoregulatory vasodilatation to CO_2 challenges immediately following CSDs have been demonstrated.[21,41]

Alterations in cerebrovascular activity may well be expected following major release of neurotransmitters, acidification and increases in intracellular calcium concentrations. A refractory period is present within the cortex following induction of CSD and it would also appear that a similar refractory period is observed in cerebral vascular autoregulation, although the extent and duration of changes in autoregulation are not clear. In our experiments we have been able to induce repeated CSD activity for up to 40–50 min following a single KCl stimulus.[6–8] This is associated with reproducible changes in pial artery diameter and laser Doppler flux. Even if autoregulatory processes to CO_2 are attenuated following a single CSD event, cerebrovascular reactivity in response to repeated CSD is maintained. This raises the possibility that pial reactivity can produce repeated activation of trigeminovascular afferents and release of CGRP.

CENTRAL SENSITIZATION

It is known that CSD activates sensory nerves and induces release of vasoactive sensory neurotransmitters into the pial interstitium.[44] In recent years it has been discovered that nociceptive sensory neurons once activated, have the ability to induce an increase in gain in spinal and trigeminal nuclei. This increase in gain is activity dependent and occurs via the summation of C-fibre afferent inputs, with the net result of a decrease in threshold of peripheral stimuli to evoke a response and amplification of the induced response. Summation of C-fibre input can be achieved at frequencies of stimulation of 0.5 Hz and of duration approximately 10 s. Clearly, plasticity of phenotype of sensory neurons is an essential prerequisite for development of central sensitization. It has been

suggested by Woolf[47] that CSD stimulation of trigeminal afferents may induce a central sensitization which is maintained by further afferent input from sensitized peripheral nerves. Indeed Moskowitz et al[52] showed that following induction of neocortical spreading depression there was increased expression of c-fos-like immunoreactivity in the trigeminal nucleus caudalis (TNC), demonstrating a clear association between CSD and nociceptive processing. However, apparently contradictory studies have recently been published. Ingvardsen et al[44] studied c-fos expression in the TNC of halothane anaesthetized rats following elicitation of CSD activity with repeated injections of 1 M KCl or NaCl. The authors observed no positive correlation between number of CSDs and fos-positive cells in the TNC, but a linear relationship between the number of NaCl or KCl injections. The authors concluded that in this study, c-fos expression in the TNC was primarily due to a hyperosmolar effect of the solutions and not episodes of CSD. However, there may be several methodological caveats to be considered. The insertion of the glass micropipettes for injection of the solutions into the cortex induced a stab wound and elicited CSDs. This stab wound is not reproducible between or within animals in terms of c-fos expression, and therefore c-fos baselines will be different. It would also be interesting to correlate the total 'area under the curve' (millivolts) of direct current depolarizations with c-fos expression, as amplitude and duration of individual depolarizations differ, and therefore relationships between number of CSD depolarizations and TNC c-fos expression may be too simplistic an analysis. Additionally, it may be expected that with increasing cortical depolarization, c-fos expression in the TNC may tend towards a maxima, therefore it may be inappropriate to assess this relationship in terms of a linear correlation.

CSD has been demonstrated to induce expression of many other nuclear transcription factors, in particular those of the creb, jun and krox families, albeit in the cerebral cortex.[45] This observation is particularly important given the proposed role of krox proteins as stabilizers of long-term potentiation and enhancers of synaptic efficacy, a mechanism clearly involved in the establishment of central sensitization.[46] It is interesting to speculate whether krox expression would occur in the TNC following CSD induction. If expression did occur, one might propose that krox expression would give a clearer demonstration of a pathological nociceptive input to the TNC from cortical structures than measurement of c-fos alone.

CSD AND INFLAMMATION

Potassium chloride-induced parietal cortex CSD has been demonstrated to induce reactive gliosis, as evidenced by the increased expression of glial fibrillary acidic protein (GFAP) message in the cortex and hippocampus.[47] In this study the time course of increased expression of GFAP mRNA reached a maximum of 24 hours post KCl application in the ipsilateral hippocampus, but was delayed in the cortex reaching a maximum of 4 days post application. Further studies by Bonthius et al[48] and Caggiano and Kraig[49] indicated that manipulating the extracellular ionic composition was unlikely to induce GFAP upregulation, but rather eicosanoid and NO release were the most probable mediators. Interestingly, it would appear that microglia are more sensitive to NO and eicosanoid GFAP induction than astrocytes. However, CSD can

induce expression of nNOS in astrocytes during reactive gliosis at 6 hours post CSD initiation.[59] Increased expression of other proteins involved in the inflammatory cascade have also been noted. Changes in Cox-2 mRNA expression have also been shown to occur following spreading depression.[51,62]

TRIGGERING OF CSD

The initiation of CSD activity in the migraineous cortex remains a matter of debate. Obrenovitch and Urenjak[53] have proposed that CSD is initiated through an extracellular accumulation of K^+, as the initial event inducing an exocytosis of presynaptic glutamate and the removal of Mg^{2+} block from NMDA channels on the postsynaptic membranes. The authors note that whilst stimulation of glutamate neurotransmission is a requirement for CSD initiation, other processes may also be implicit such as gap junction patency. The mechanism of inappropriate K^+ ion homeostasis in this model has yet to be addressed. Extracellular K^+ buffering in the brain is primarily by glial cells and involves contributions of several mechanisms including intracellular accumulation via K^+ channels, Na^+K^+ATPase, furosemide sensitive $Na^+K^+2Cl^-$ cotransporters and extracellular diffusion of transcellular K^+ migration.

Studies by Read et al[7] demonstrate that furosemide pretreatment in a cat model of K^+-stimulated CSD, inhibited CSD generation. The mechanism of inhibition of regenerative CSD activity by furosemide is unknown. It may represent a disruption in K^+ drive, or equally non-specific effects of furosemide such as inhibition of glutamate or γ-aminobutyric acid receptors. However, it may be that furosemide inhibits CSD activity by a cell volume dependent mechanism. Changes in extracellular space are known to modulate 'normal' activity and contribute to pathological excitation of the central nervous system. Indeed, hyperosmicity and hence cell swelling, has been shown to trigger CSD. Conversely therefore, hyperosmicity and cell shrinkage may inhibit CSD generation.[54] This hypothesis is not without precedent. In models of status epilepticus, hyperosmotic conditions such as intravenous mannitol infusion modulate seizure activity,[55] an effect identical to hyperosmotic intervention with intravenous urea in the clinic. Studies by Hochman et al[56] have demonstrated that furosemide inhibits epileptiform activity via a nonsynaptic mechanism. The authors propose that this inhibition maybe via a modulation of glial cell volume changes, the net result of which is an attenuated excitation of the central nervous system.

Genesis of CSD activity in migraineurs could be a manifestation of inappropriate ion homeostasis via channelopathies. This proposal is at present circumstantial, however not without precedent. Linkage analysis by Ophoff et al[57] has confirmed that familial hemiplegic migraine is caused by missense mutations in the brain specific *P/Q*-type Ca^{2+} channel gene CACNL1A4. The electrophysiology of this allelic disorder, has yet to be described although the autosomal dominant mode of inheritance may suggest gain of function.[58] It remains likely that the initial trigger may be multifactorial with many possibilities including altered ionic homeostasis, altered glutamate metabolism and environmental cues (Figure 8.2).

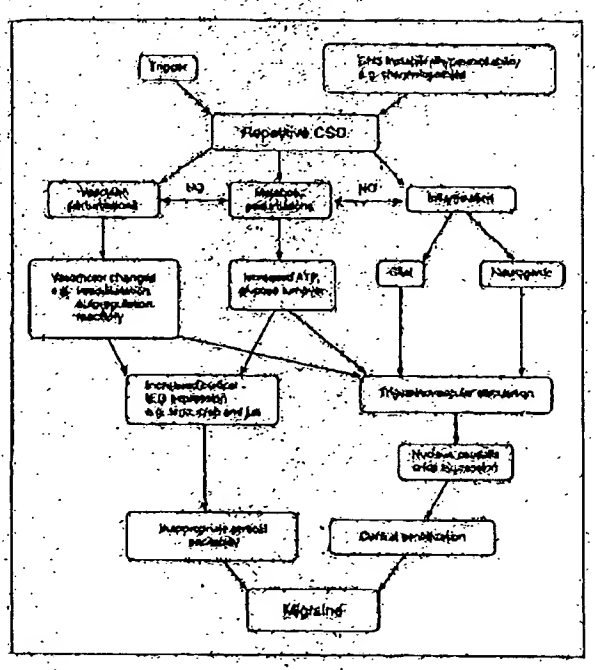

Fig. 8.2 The CSD continuum

CONCLUSIONS

It is apparent on review of CSD studies that changes in metabolic, vascular and gene expression observed in experimental CSD are complex and have a number of correlates in the clinic in migraine with and without aura. Migraine is triggered by a variety of environmental cues and it seems likely that the primary event is a metabolic disturbance, resulting in a central sensitization of the trigeminovascular fibres. Cortical spreading depression provides a link between metabolic disturbance, vasculature dilatation, nitric oxide release and alteration of gene expression.

Normalizing a pathophysiological cortical metabolic state by intervention of CSD is therefore a valid pharmaceutical target. By treating the overall process and not just offering symptomatic relief by current treatments, migraine therapy may be approaching a new era, where causative relationships to other neurological disorders, for example stroke,[60,61] can also be addressed.

REFERENCES

1 Leao AAP. Spreading depression of activity in the cerebral cortex. *J Neurophysiol* 1944; 7:359–90.
2 Kempski O, von Rosen S, Weigt H, et al. Glial ion transport and volume control. *Ann NY Acad Sci* 1991; 633:306–17.
3 Marshall WH. Spreading cortical depression of Leao. *Physiol Rev* 1959; 39:239–79.
4 Gardner-Medwin AR. Magnetometry and magnetic resonance imaging: complementary approaches to the spreading depression issue in migraine. In: Clifford Rose F, ed., *Towards Migraine 2000, Developments in Neurology*. Amsterdam: Elsevier Science, 1996; Volume 12: 163–7.
5 Read SJ, Smith MI, Hunter AJ, Parsons AA. The dynamics of nitric oxide release measured directly and in real time following repeated waves of cortical spreading depression in the anaesthetised cat. *Neurosci Lett* 1997; 232:127–30.
6 Read SJ, Smith MI, Hunter AJ, Parsons AA. Enhanced nitric oxide release during cortical spreading depression following infusion of glyceryl trinitrate in the anaesthetised cat. *Cephalalgia* 1997; 17:159–65.
7 Read SJ, Smith MI, Benham CD, et al. Furosemide inhibits regenerative cortical spreading depression in anaesthetized cats. *Cephalalgia* 1997; 17:826–32.
8 Piper RD, Lambert GA. Inhalation anaesthetics inhibit spreading depression: relevance to migraine. *Cephalalgia* 1996; 16:87–92.
9 Shinohara M, Dollinger B, Brown G, et al. Cerebral glucose utilisation: local changes during and after recovery from spreading cortical depression. *Science* 1979; 203:188–90.
10 Csiba L, Paschen W, Mies G. Regional changes in tissue pH and glucose content during cortical spreading depression in rat brain. *Brain Res* 1985; 336:167–70.
11 Lauritzen M, Diemer NH. Uncoupling of cerebral blood flow and metabolism after single episode of cortical spreading depression in the rat brain. *Brain Res* 1986; 370:405–8.
12 Gjedde A, Hansen AJ, Quistorff B. Blood brain glucose transfer in spreading depression. *J Neurochem* 1981; 37:807–12.
13 Mraovitch S, Calando Y, Goadsby PJ, Seylaz J. Subcortical cerebral blood flow and metabolic changes elicited by cortical spreading depression in rat. *Cephalalgia* 1992; 12:137–41.
14 Mies G, Paschen W. Regional changes of blood flow, glucose and ATP content determined from brain sections during a single passage of spreading depression in the rat brain cortex. *Exp Neurol* 1984; 84:249–58.
15 Lauritzen M, Hansen AJ, Kronborg D, Wieloch T. Cortical spreading depression is associated with arachidonic acid accumulation and preservation of energy charge. *J Cereb Blood Flow Metab* 1990; 10:115–22.
16 Atkinson DE. The energy charge of the adenylate pool as a regulatory parameter. Interaction with feedback modifiers. *Biochemistry* 1968; 7:4030–4.
17 Barbiroli B, Montagna P, Cortelli P, et al. Abnormal brain and muscle energy metabolism shown by 31P magnetic resonance spectroscopy in patients affected by migraine with aura. *Neurology* 1992; 42:1209–14.
18 Welch KMA, Levine SR, D'Andrea G, et al. Preliminary observations on brain energy metabolism in migraine studied by phosphorus-31 NMR spectroscopy. *Neurology* 1989; 39:538–41.
19 Siesjo BK. Calcium mediated processes in neuronal degeneration. *Ann NY Acad Sci* 1994; 747:140–61.
20 Gido G, Kristian T, Katsura K, Siesjo BK. The influence of repeated spreading depression-induced calcium transients on neuronal viability in moderately hypoglycemic rats. *Exp Brain Res* 1993; 97:397–403.
21 Lacombe P, Sercombe R, Correze JL, et al. Spreading depression induces prolonged reduction of cortical blood flow reactivity in the rat. *Exp Neurol* 1992; 117:278–86.
22 Lauritzen M. Long-lasting reduction of cortical blood flow of the rat brain after spreading depression with preserved autoregulation but impaired CO_2 response. *J Cereb Blood Flow Metab* 1984; 4:546–54.
23 Piper RD, Lambert GA, Duckworth JW. Cortical blood flow changes during spreading depression in cats. *Am J Physiol* 1991; 261:H96–102.
24 Olesen J. Cerebral and extracranial circulatory disturbances in migraine. Pathophysiological implications. *Cerebrovasc Brain Metab Rev* 1991; 3:1–28.
25 Woods RP, Iacoboni M, Mazziotta JC. Bilateral spreading cerebral hypoperfusion during spontaneous migraine headache. *N Engl J Med* 1994; 331:1689–92.
26 Andersson JLR, Muhr C, Lilja A, et al. Regional cerebral blood flow and oxygen metabolism during migraine with and without aura. *Cephalalgia* 1997; 17:570–9.
27 Weiller C, May A, Limmroth V, et al. Brain stem activation in spontaneous human migraine attacks. *Nature Med* 1995; 1:658–60.
28 Gardner-Medwin AR, van Bruggen N, Williams SR, Ahier RG. Magnetic resonance imaging of propagating waves of spreading depression in the anaesthetised rat. *J Cereb Blood Flow Metab* 1994; 14:7–11.
29 Gao Y, Vikingstad E, Aurora S, Welch KMA. Functional MRI of visually triggered headache: activation, suppression and propagation of the BOLD effect. *J Cereb Blood Flow Metab* 1997; 17(Suppl 1):S176.
30 Duckrow RB. A brief hypoperfusion precedes spreading depression if nitric oxide synthesis is inhibited. *Brain Res* 1993; 618:190–5.
31 Wahl M, Schilling L, Parsons AA, Kaumann A. Involvement of calcitonin gene-related peptide (CGRP) and nitric oxide (NO) in the pial artery dilatation elicited by cortical spreading depression. *Brain Res* 1994; 637:204–10.
32 Meng W, Colonna DM, Tobin JR, Busija DW. Nitric oxide and prostaglandins interact to mediate arteriolar dilation during cortical spreading depression. *Am J Physiol* 1995; 269:H176–81.
33 Zhang ZG, Chopp M, Maynard KI, Moskowitz MA. Cerebral blood flow changes during spreading depression are not altered by inhibition of nitric oxide synthesis. *J Cereb Blood Flow Metab* 1994; 14:939–43.
34 Iadecola C, Pelligrino DA, Moskowitz MA, Lassen NA. Nitric oxide synthase inhibition and cerebrovascular regulation. *J Cereb Blood Flow Metab* 1994; 14:175–92.
35 Peterson DA, Peterson DC, Archer S, Weir EK. The non specificity of specific nitric oxide inhibitors. *Biochem Biophys Res Commun* 1992; 187:797–801.
36 Malinski T, Bailey F, Zhang ZG, Chopp M. Nitric oxide measured by a porphyrinic microsensor in rat brain after transient middle cerebral artery occlusion. *J Cereb Blood Flow Metab* 1993; 13:355–8.
37 Read SJ, Parsons AA. Spreading depression and cortical nitric oxide release. *J Cereb Blood Flow and Metab* 1997; 17(Suppl 1):S548.
38 Olesen J, Iversen HK, Thomsen LL. Nitric oxide supersensitivity: a possible molecular mechanism of migraine pain. *NeuroReport* 1993; 4:1027–30.
39 Iversen HK, Olesen J, Tfelt-Hansen P. Intravenous nitroglycerin as an experimental model of vascular headache. *Pain* 1989; 38:17–24.
40 Olesen J, Thomsen LL, Iversen HK. Nitric oxide is a key molecule in migraine and other vascular headaches. *Trends Pharmacol Sci* 1994; 15:149–53.
41 Florence G, Bonvento G, Charbonne R, Seylaz J. Spreading depression reversibly impairs autoregulation of cerebral cortical blood flow. *Am J Physiol* 1994; 266:R1136–40.
42 Moskowitz MA, Nozaki K, Kraig RP. Neocortical spreading depression provokes the expression of c-fos protein-like immunoreactivity within trigeminal nucleus caudalis via trigeminovascular mechanisms. *J Neurosci* 1993; 13:1167–77.
43 Woolf CJ. Central sensitization: implications for the pathogenesis of headache. In: Clifford Rose F, ed., *Towards Migraine 2000. Developments in Neurology*. Amsterdam: Elsevier Science, 1996; Volume 12: 173–81.
44 Ingvardsen BK, Laursen H, Olsen UB, Hansen AJ. Possible mechanism of c-fos expression in trigeminal nucleus caudalis following cortical spreading depression. *Pain* 1997; 72:407–15.
45 Herdegen T, Sandkuhler J, Gass P, et al. JUN, FOS, KROX and CREB transcription factor expression in the rat cortex: basal expression and induction by spreading depression and epileptic seizures. *J Comp Neurol* 1993; 333:271–88.
46 Hughes P, Dragunow M. Induction of immediate early genes and the control of neurotransmitter-regulated gene expression within the nervous system. *Pharmacol Rev* 1995; 47:133–78.
47 Bonthius DJ, Steward O. Induction of cortical spreading depression with potassium chloride upregulates levels of messenger RNA for glial fibrillary acidic protein in cortex and hippocampus: inhibition by MK-801. *Brain Res* 1993; 618:83–94.
48 Bonthius DJ, Lothman EW, Steward O. The role of extracellular ionic changes in upregulating the mRNA for glial fibrillary acidic protein following spreading depression. *Brain Res* 1995; 674:314–28.
49 Caggiano AO, Kraig RP. Eicosanoids and nitric oxide influence induction of reactive gliosis from spreading depression in microglia but not astrocytes. *J Comp Neurol* 1996; 369:93–108.
50 Caggiano AO, Kraig RP. Astrocytes express neuronal nitric oxide synthase following spreading depression. *J Cereb Blood Flow Metab* 1997; 17(Suppl 1):S552.
51 Caggiano AO, Breder CD, Kraig RP. Long term elevation of cyclo-oxygenase 2, but not lipo-oxygenase, in regions synaptically distant from spreading depression. *J Comp Neurol* 1996; 376:447–62.
52 Miettinen S, Fusco FR, Yrjanheikki J, et al. Spreading depression and focal brain ischemia induce cyclo-oxygenase-2 in cortical neurones through N-methyl-D-aspartic acid receptors and phospholipase A2. *Proc Natl Acad Sci USA* 1997; 94:6500–5.

53 Obrenovitch TP, Urenjak J. Altered glutamatergic transmission in neurological disorders: from high extracellular glutamate to excessive synaptic efficacy. *Prog Neurobiol* 1997; 51:39–87.

54 Chebabo SR, Hester MA, Aitken PG, Somjen GG. Hypotonic exposure enhances synaptic transmission and triggers spreading depression in rat hippocampal tissue slices. *Brain Res* 1995; 695:203–16.

55 Baran H, Lassmann H, Sperk G, et al. Effect of mannitol treatment on brain neurotransmitter release markers in kainic acid-induced epilepsy. *Neuroscience* 1987; 21:679–84.

56 Hochman DW, Baraban SC, Owens JWM, Schwarcz R, Postema PA. Dissociation of synchronization and excitability in furosemide blockade of epileptiform activity. *Science* 1995; 270:99–102.

57 Ophoff RA, Terwindt GM, Vergouwe MN, et al. Familial hemiplegic migraine and episodic ataxia type-2 are caused by mutations in the Ca^{2+} channel gene CACNL1A4. *Cell* 1996; 87:543–52.

58 Luebke JI, Dunlap K, Turner TJ. Multiple calcium channel types control glutamatergic synaptic transmission in the hippocampus. *Neuron* 1993; 11:895–902.

59 Ording JE, Hsieh P, Romero J, et al. Migraine and subsequent risk of stroke in the Physicians' Health Study. *Arch Neurol* 1999; 52:129–34.

60 Merikangas KR, Fenton BT, Cheng SH, et al. Association between migraine and stroke in a large-scale epidemiological study of the United States. *Arch Neurol* 1997; 54:362–8.

61 Parsons AA, Read P, Smith MI, et al. Cortical spreading depression: a missing link? In: Clifford Rose F, ed. *Towards Migraine 2000. Developments in Neurology*. Amsterdam: Elsevier Science, 1996: Volume 12: 153–61.

9 Neurogenic inflammation: relation to novel antimigraine drugs

Richard J Hargreaves, David J Williamson, Sara L Shepheard

INTRODUCTION

The neural events that link migraine trigger factors to the initiation of an attack are relatively poorly understood but considerably more is known about the pathophysiology of migraine headache pain. Our understanding of these pathophysiological mechanisms has been enhanced by increased knowledge of the pharmacology of the trigeminovascular system as a result of the introduction of highly effective acute antimigraine drug therapies.

The brain has a sparse sensory innervation and it is the superficial capsule structures comprising the meninges that are the most significant pain-producing intracranial tissues.[1,2] The meningeal blood vessels are highly responsive to many vasoactive substances[3] and their mechanical or electrical stimulation is known to produce intense head pain that is mediated by the trigeminal nervous system.[4,5] For many years a vascular hypothesis held that migraine was primarily a disorder of the cranial vasculature and proposed that the pain of headache occurred as a result of perivascular trigeminal sensory nerve activation by inappropriate vasodilatation or opening of arteriovenous anastomoses in the cranial circulation.[6] This theory explained the antimigraine efficacy of vasoconstrictor agents such as the ergots although it did not account for the lack of activity of other powerful constrictors such as norepinephrine. This discrepancy led to the idea that other factors must be involved and focused thinking upon the trigeminal sensory nerves that become activated when the intracranial blood vessels dilate.[7]

The sensory nerves innervating pain-producing extracerebral intracranial blood vessels arise from the first division of the trigeminal nerve (Vth cranial nerve), the ophthalmic branch. The neuronal cell bodies giving rise to these peripheral sensory fibres are found within the trigeminal ganglia. These ganglia are located bilaterally however, innervation is predominantly unilateral and widespread, an anatomical arrangement that could account for the unilateral nature of migraine headache.[8,9]

The perivascular trigeminal sensory nerve fibres contain several vasoactive pro-inflammatory substances most notably the peptides substance P, neurokinin A and calcitonin gene-related peptide (CGRP).[10–12] Substance P and neurokinin A primarily cause increased blood vessel permeability (with relatively transient vasodilatation) whereas CGRP produces a profound and long-lasting vasodilatation without increasing blood vessel permeability. The effects of these vasoactive peptides are mediated

Brain Research, 614 (1993) 45–51

BRES 18899

Self-sustained spreading depressions in the chicken retina and short-term neuronal–glial interactions within the gray matter neuropil

V.M. Fernandes de Lima [a], D. Scheller [b], F. Tegtmeier [b], W. Hanke [a] and W.R. Schlue [c]

[a] *Institute of Zoophysiology / 230, Hohenheim University, W-7000 Stuttgart 70 (FRG),* [b] *Janssen Research Foundation CNS-Pharmacology, W-4040 Neuss 21 (FRG) and* [c] *Institute of Zoophysiology I, Düsseldorf University, W-4000 Düsseldorf (FRG)*

(Accepted 5 January 1993)

Key words: Spreading depression; Retina; Müller cell; Neuronal–glial interaction

The chicken retina is an accessible piece of intact gray matter in which a self-sustained form of the 'Spreading Depression' (SD) wave can be easily elicited and recorded for many hours with double barrel ion-sensitive electrodes in the extracellular space. The blockade of glial (Müller) cell potassium channels with barium chloride added to the perfusing Ringer depressed both the negative potential shift typical of SDs and the velocity of spread. Moreover, there was separation of the extracellular increase of potassium and the drop in the extracellular potential: the peak of the potassium wave was increased, as well as its duration whereas the potential wave could be depressed to zero or even inverted to positive. By contrast the transient extracellular calcium drop could not be separated from the extracellular potential wave but appeared related to it: no transient calcium drop was observed when the negative potential was completely depressed or inverted. Both, the amplitude of the extracellular potential and extracellular calcium activity appeared to be important factors controlling the velocity of spread.

INTRODUCTION

Spreading depression of electroencephalographic activity[16], is a wave like phenomenon that can be elicited in different parts of gray matter among which the vertebrate retina[13]. In this tissue, marked optical changes are concomitant with the massive increase in the extracellular potassium concentration and slow negative shift typical of SDs. One of the advantages of the retinal preparation is the direct observation of the two dimensional spread. Another advantage is the laminar structure with well defined neuropils and cell body layers. In the avascular chicken retina, the inner plexiform layer is especially large (100 μm width). It consists of only one type of glial cells, the Müller cells. and synaptic terminals. The glial processes surround the synaptic terminals and fill most of the neuropil space. The end-feet of the same Müller cells form the inner limiting membrane, which separates the extracellular space of nervous tissue from the vitreous humour. Thus, in this preparation, one can have access to a simplified neuropil with only synaptic terminals and one type of glia. This laminar structure with well separated cell bodies and neuropils gives rise to sharp field potentials when massive population responses are elicited either by a flash of light (electroretinogram) or during the spreading depression wave[9,20,21,24,26]. As is the case in the hippocampus, one can easily position an electrode by following the field profile.

Intense neural activation promotes release of potassium to the extracellular space. The role of glia in the potassium clearance and generation of field potentials in the retina has been the subject of studies for two decades[21]; (for reviews see refs. 10 and 26). Neural activation, either light evoked or during SDs, increases extracellular potassium in the two plexiform layers of the retina and lead to influx of potassium into Müller cells[23,24,25]. Very recently, we were able to record channel activities in presumably ganglion cell layer cell bodies and glia end feet membranes during SDs in intact retinas[14]. Both neural and glial potassium channels increased activity during wave passage. The duration of increased activity in glial channels was coincident with the slow negative shift. We hypothesized,

Correspondence: V.M. Fernandes de Lima, Universität Hohenheim, Institut für Zoophysiologie / 230, Garbenstraße 30, W-7000 Stuttgart 70 - Hohenheim, FRG. Fax: (49) (711) 459 2795.

therefore, that during SD massive neuronal activation in the neuropil challenges the glial homeostatic mechanisms and this interaction in turn must give rise to the negative potential shift and spreading phenomenom.

To test that, barium was applied. Barium is a well known blocker of glial K-channels (v.g. refs. 2 and 6) and in this paper we relate the results of a series of experiments in wich a form of self-sustained SDs, the circling preparation[20], was utilized to test the effect of glial channel blockade on the negative shift and extracellular potassium dynamics.

MATERIALS AND METHODS

Chickens from an age of 15 to 35 days were killed by decapitation and the eye cups dissected from the skull immediately. The anterior chamber was cut off at the equator and the humour vitreous removed. The posterior chamber was then immersed in a Ringer solution containing: 100 mM NaCl; 6 mM KCl; 1 mM $MgSO_4$; 1 mM $CaCl_2$; 1 mM NaH_2PO_4; 30 mM NaH_2CO_3 and 30 mM glucose. The solution was bubbled with a mixture of 95% O_2 and 5% CO_2 to a final pH of 7.4. A circular cut was performed in order to create a ring of continuous tissue and the eye cup placed in a perfused chamber with 5 ml internal volume, maintained at constant temperature of 30°C. The chamber was perfused continously with a flow velocity of 1.5 ml/min (see Fig. 1 of ref. 20 for more details). One SD was elicited mechanically using a fine tungsten needle (100 μm diameter) close to the narrowest part of the ring and two wave fronts were obtained. One of these was stopped using a Ringer solution with 10 mM $MgSO_4$ spread over the retina with a glass needle and the remaining wavefront was 'trapped' within the ring[20].

Single or double micropippetes (2–3 μm tip diameter) were used for recording of the slow potential shift and extracellular ion activities during the experiments. Details about the microelectrodes construction and calibrations have been published[8,30]. Potassium activity was measured with the Fluka 1 B 60398 ionophore and the calcium activity with the Fluka 1 B 21191 ionophore. Electrode calibrations were performed at the begining and at the end of the experiments in the following way: after the usual calibration proceeding[8,30], electrodes with responses close the expected Nerstian slopes were positioned at the center of the chamber and calibrated again with the slow rate of change used in the experiments. The slopes were in all cases smaller than the previous ones and these slopes were the ones used to estimate the ionic activity. For the electrophysiological recordings a high impedance dual differential electrometer was used (WPI,Inc. FD 223), both channels were continously recorded on a Gould 2200 S pen recorder and on a dual beam oscilloscope. The bathing solution in the measuring chamber was grounded (with an Ag/AgCl wire electrode). The optical signal and the general transparency of the retina were observed with naked eye.

RESULTS

Fig. 1 shows the typical periodic recording of circling SDs registered with double barreled DC- and ion-sensitive electrode within the neuropil. At 30°C and with an outer ring of intact retinal tissue of 15 mm length, the repetitive waves are separated by a period of about 5 min (velocity 3 mm/min) and the negative slow potential shift (NSPS) is typically around 10 mV.

Switching the perfusion solution to a Ringer in which 2 or 4 mM barium chloride was added, affected several parameters in the experiments in a consistent manner ($n = 7$ retinas and 15 barium pulses). First, there was considerable slowing down of the velocity of SDs. Second, there was reduction of the amplitude of the NSPS (Fig. 1). In this and all other figures, the begining of the bar that indicates the pulse of barium Ringer, is set at 4 min after the actual switch and indicates the time when the ion-sensitive channel positioned at the center of the chamber reached a plateau phase during the calibration procedure. The effect of barium outlasted the pulse in all experiments. Partial recovery of the amplitude was always present. The recovery of amplitude was usually complete after 40

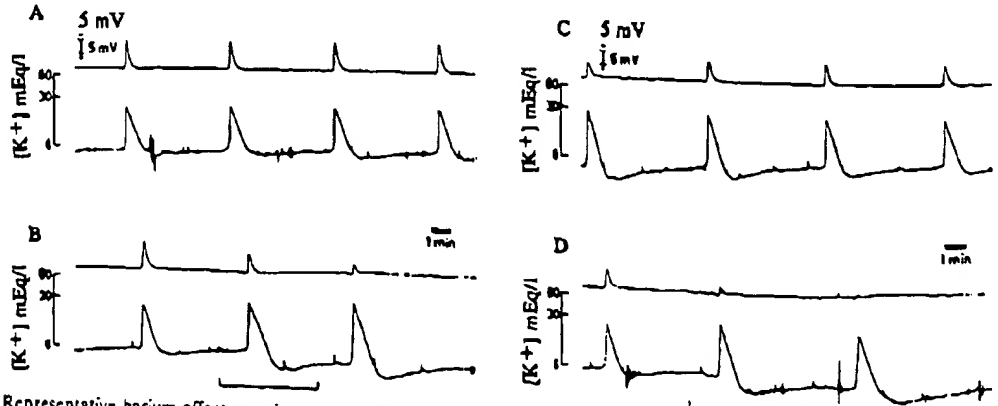

Fig. 1. Representative barium effect experiment. A: control records with double barrel potassium sensitive electrodes. Upper row extracellular potential signal and lower row extracellular potassium activity in four successive SDs in circling preparation. Interval between waves around 5 min, potential amplitude −10 mV, peak potassium signal 27 mEq/l; B: pulse of 4 min 2 mM barium chloride added to perfusing Ringer. Interval after the third wave increased to 6.6 min. Amplitude of negative potentials 10, 6.5 and 4 mV, respectively. Potassium peaks: 27, 31 and 41 mEq/l; C: 40 min later partial recovery of both amplitude and wave intervals. Potential amplitude −6.5 mV peak potassium 25 mEq; D: second pulse with 4 mM barium chloride for 6 min. Potential amplitudes 6.5, 2.5 and 1 mV. Peak potassium 25, 31.5, 31.5 mEq/l. After the third wave the interval increased to 27 min, a fivefold decrease in the spread velocity.

min. In about the same time, the propagation velocity recovered either partially or completely. In three out of five trials with 4 mM barium, the NSPS was inverted from negative to positive. These positive SDs had a low amplitude (2–2.5 mV) and were slow compared with the sudden onset of the negative shifts (Fig. 3). In two of these trials the propagation velocity decreased 5-fold and in the three others, the circling of SD stopped altoghether although the retina remained susceptible to mechanical stimulation.

The extracellular potassium dynamics both during waves and in the interval between successive waves was also markedly affected. The peak value of potassium increased (from 27 to 41 mEQ and from 25 to 32 mEq, respectively in parts B and D of the experiment shown in Fig. 1), the rate of recovery of the potassium wave was slowed down and the 'undershoot' phase was accentuatted. The baseline potassium levels fell from 6 to 4 mEq and was maintained low for several minutes after washing out of barium. This fall in baseline potassium level was accompanied by a small positive shift of the potential record baseline.

The extracellular calcium activity during SD dropped by as much as two log units (Fig. 4) with a complex time course of recovery with rapid and slow phases (see Figs. 2 and 4). Upon barium application, the calcium signal was affected in a fashion similar to the NSPS: the stronger the depression in amplitude of the NSPS, the smaller the drop in calcium and the slower the recovery. But this relationship was by no means linear.

In summary: Barium depressed the amplitude of the NSPS. The potassium wave could be dissociated from the field potential wave. The calcium drop, by contrast, could not be separated from the NSPS.

In the course of the experiments we observed 47 'spontaneous' SDs in which the SD clearly could be identified optically, but the field potential was positive: 15 were recorded toghether with potassium and 32 together with calcium electrodes (Fig. 5). The potassium signal in these waves had the slow recovery time course observed in the barium experiments and in all the waves recorded with calcium electrodes, no transient drop in calcium was seen. The calcium signal was also slow in onset, small in amplitude and recovered within 3 to 4 min. These instances of 'spontaneous' positive SDs were in line with the observation that the initial fast drop of the calcium signal was related to the fast phase of the negative potential drop. This suggests that the effect of barium on the propagation velocity could be caused primarily by calcium dependend mechanisms. In order to clarify the relationship between extracellular calcium, fast calcium drop and velocity of SD, we lowered the calcium concentration in the Ringer from 1 to 0.1 mM. In all of these experiments, the velocity of SDs was slowed down ($n = 6$ retinas, 7 pulses). In some cases the amplitude of the NSPS at first increased and then decreased during the low calcium pulse (Fig. 2). The extracellular calcium activity subsequent to the change in concentration in the perfusion Ringer occurred very slowly in contrast with the well known fast equilibrium with potassium pulses. It can take as long as 5 min after changing the bath solution for the extracellular calcium activity within the neuropil to begin to fall. It takes a further 10 to 15 min to decrease very slowly to a level of 0.5 to 0.6 mM. Restoration of the normal calcium activity superfusion with normal Ringer required 4 to 16 min ($n = 6$ pulses). Substituting sodium chloride in the Ringer by choline

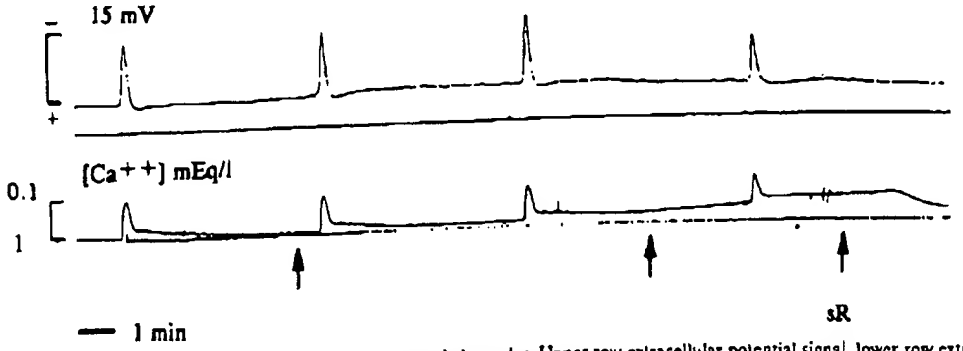

Fig. 2. Record of circling SDs experiment with calcium double barrel electrodes. Upper row extracellular potential signal, lower row extracellular calcium activity. The register of the calcium signal was made with an inverting cable such that a drop in calcium is seen as an upward deflection. Note the fast drop and the apparent two component recovery with fast and slow phases. At the first arrow, 0.1 mM calcium chloride Ringer was equilibrated at the chamber. The interval between waves increased by 0.5, 1 and 2 min and the circling stopped. The negative potential increased from 13 to 15 mV and then decreased to 10 mV in the last wave. The baseline calcium activity hardly changed in the first 5 min after lowering perfusing calcium and then began a very slow decrease. This decrease was accelerated when choline chloride Ringer also with 0.1 mM calcium was equilibrated in the chamber (second arrow). The baseline calcium level was about 0.7 mEq/l after 10 min of perfusion, about 0.5 mEq/l just before the last wave and at the end of pulse 0.2 mEq/l. Recovery to 0.9 mM extracellular calcium level was fast upon reintroduction of both calcium and sodium 'standard' levels in the Ringer (third arrow).

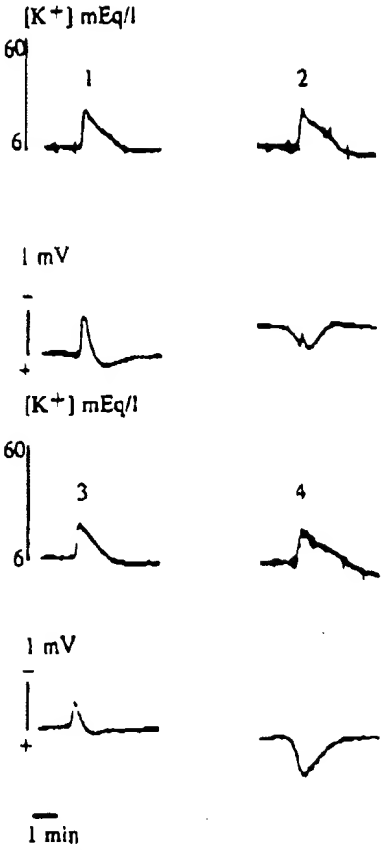

Fig. 3. Inversion of field potential with barium pulses. All four waves shown in the figure belong to the same experiment. 1 and 3 are controls and 2 and 4 were recorded during perfusion with barium chloride (4 mM). Waves 1 and 2 were recorded during circling and 3 and 4 were mechanically elicited. Time interval between the end of the first pulse (during wich wave 2 was recorded) and the recording of wave 3 (recorded just before the second pulse) was 1 h and 20 min.

chloride brought the extracellular calcium activity to 0.2 mM (2 experiments 3 pulses) with 10 to 15 min pulses.

In summary: when the NSPS was depressed or inverted to positive, the fast transient drop of calcium was not present although SD was optically visible. Extracellular calcium activity is an important factor controlling propagation velocity. Reducing extracellular sodium impaired control mechanisms of calcium homeostasis.

DISCUSSION

Barium pulses blocked the fast rising negative extracellular potential typical of SDs. By contrast, the increase in the extracellular potassium concentration was not blocked. Barium is a well known blocker of glia potassium channels[2,6]. Three conclusions are in agreement with these findings:

first, the best candidates for the source of the extracellular potassium are the synaptic terminals (besides the glial menbrane there is nothing else in this neuropil);

second, the negative potential shift is due to channel activity in the glia menbrane;

third, the density of these channels must be high as indicated by the size of the extracellular potential drop, caused by the resultant sink of extracellular current.

Barium pulses also affected the baseline potassium level between successive circling waves. A similar drop in the baseline extracellular potassium was seen in the cortex[6] In our records this baseline fall in potassium was accompanied by a small positive shift of the baseline potential. The simplest interpretation of these results is to attribute both changes to the Na/K ATPase that it is present the terminals as well as in glia neuropil menbranes. Given that most of the menbrane within the neuropil is glial[10]; the Müller cell Na/K ATPase is accelerated by increases in the extracellular potassium levels and its activity can continue even in

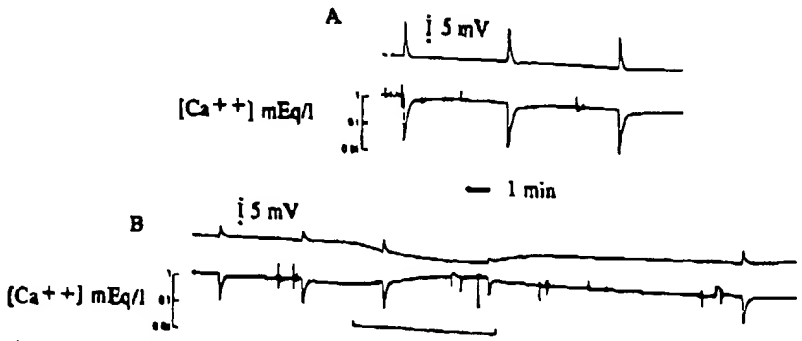

Fig. 4. Exemple of barium experiment with recording of extracellular calcium activity. A: circling wave at the begining of the experiment. Upper row extracellular potential and lowe row extracellular calcium activity. B: the lenght of the bar indicates the duration of the barium pulse. This part of the figure shows the second barium pulse of this experiment. Note the smaller amplitude in both signals: the potential signal is one third of the control amplitude and the calcium signal amplitude is halved. The last wave in part B was mechanically elicited.

low Na or Na-free solutions[28,29]; glial pump activity is higher in glia than in neuronal menbranes[35], thus it follows that the effects seen are very likely to be glial effects.

If we put togheter these results with the results of a parallel series of 'patch-clamping' experiments in the intact retina as well as in patchs from acutely isolated Müller cells[14], the interplay between neurons and glia pumps and channels during SDs appears as follows: a massive release of potassium from terminals transiently overcomes the pump uptake. The glial menbrane potential that just before the wave was in the potassium equilibrium potential, deviates from it and electrochemical gradient pushes potassium into glia, giving rise to the extracellular negative potential drop, and in a few seconds the glia will be again in equilibrium. The pump uptake brings it away from electrochemical equilibrium potential and then potassium will leave glia through the channels. We have found that the open state probability of Müller cell potassium channels is very high for the entire range of physiological potentials[14]. Thus, not only during waves but in the period between successive waves as soon as potassium enters glia trough active transport, there is a tendency to leave it through the high conductance of the channels. Potassium will only enter glia through channels in the situations when the glia uptake is overcome.

This model predicts that non-specific blockers of potassium channels that would affect the synaptic terminals membrane as well, will depress the amplitude of both the potassium and potential wave. It also predicts that in the presence of the Na/K ATPase blocker ouabain, the rise in the extracellular potassium must be very fast and that very high concentrations of potassium will be reached in the extracellular space.

Spatial transfer of considerable amount of potas-

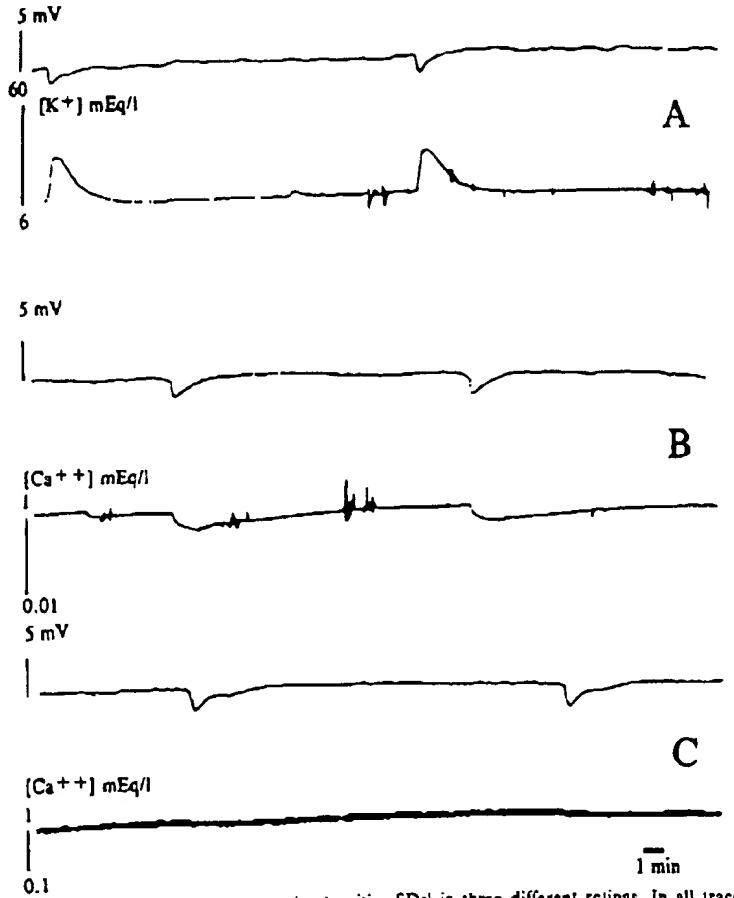

Fig. 5. A, B and C show examples of 'spontaneously' occurring 'positive SDs' in three different retinas. In all traces upper row shows the extracellular field potential and the lower row the extracellular ion activity. In each experiment the recordings correspond to the position within the retina in which either the ion-sensitive channel (Potassium electrode experiment) or the field potential was maximal (calcium electrode experiment).

sium has been proposed to play a key role in propagating activity[11,12]. Our results are not compatible with this concept.

The general technique of applying current through the tissue, measuring the potential drop and calculating current[11,12] was applied to the retina[15]. Potassium in the vitreous was confined to a distance of 200 μm in these experiments. When approaching the retina from the vitreous surface in a circling wave experiment, one begins to measure a potassium signal when the electrode is within 200 μm range. At a distance around 50 μm the potassium wave in the vitreous do not outlast the undershoot of subsequent waves recorded within the neuropil. Again it appears that as soon as potassium leaves glia channels it is pumped back by the accelerated Na/K ATPase that is present in the same membrane. The potassium signal in the vitreous above the inner limiting membrane was blocked by barium in these experiments[15].

Barium depressed the fast transient calcium drop in the extracellular space that accompanies SDs. In retinas in which the field potential was inverted from negative to positive, there was no fast calcium transient in the neuropil. We propose that the fast component of the calcium signal is the consequence of the opening of voltage-sensitive cation channels in the glia membrane within the neuropil. Again in the simplified situations of the chicken inner plexiform layer, only two types of membrane are present and if the depolarization of glia is one necessary condition for the calcium signal, then it follows that this macroscopic signal is very likely also glial in origin. Given that:

(a) voltage sensitive cation channels are present in glia membrane[3];

(b) depolarization of glia syncytium in culture by glutamate produces calcium waves[7];

(c) in the presence of barium, glial cells hyperpolarize and accumulate bicarbonate[2,6,31] and thus in this situation voltage-sensitive channels would remain closed, the proposed interpretation of the present experiments is again the simplest. The recovery of the extracellular baseline level also appeared to be related to the fast transient: the calcium signal with a small or absent fast phase was very slow in recovering (Fig. 5). It is known that among the several transport mechanisms involved in calcium extrusion and uptake, some are triggered by the rising of calcium itself. The electrogenic 3Na/1Ca antiport that depends on sodium gradient and can be reversed is of the type triggered by calcium transients[32]. We have observed that the fall in the baseline extracellular calcium level was accentuated if the sodium gradient was lowered in the perfusion solution.

The experiments with manipulations of calcium and sodium concentrations in the perfusion solution, extracellular ion-sensitive recordings in the neuropil, and short-term disturbances in the baseline potassium with barium perfusion, suggest that this 'in vitro' system is specially suitable for the study of the role of glial barriers in the maintenance of the microenviroment. As a matter of fact, the inner limiting membrane formed by the end-feet of the Müller cells that faces the vitreous surface is very similar to the strucuture found in the pure glial blood–brain barrier of invertebrates[1].

In summary our results clearly show that the field potential and extracellular potassium signals of the SD wave can be separated. Their close association has been frequently reported[4,5,16,17,31] and Tomita[32] showed that in the retina extracellular potential and glial intracellular potassium signals were 'mirror images' of each other. The same was shown in the turtle cerebellum[27]. The present experiments establish the synaptic terminals as the origin of the potassium and the glial membrane potassium channels as the origin of the field potential. This neuronal–glial interaction model for the SD predicts the behaviour of some macrospic variables that can be verified experimentally.

REFERENCES

1 Abbot, J., Permeability and transport of glial blood–brain barriers, *Ann. NY Acad. of Sci.*, 633 (1991) 378–394.

2 Ballany, K.P., Graphe, P. and Bruggencate, G., Ion activities and potassium uptake mechanism of glial cells in guinea pig olfactory cortx slices, *J. Physiol.*, 382 (1987) 159–174.

3 Barres, B., New roles for glia, *J. Neurosci.*, 11 (1991) 3685–3694.

4 Bures, J., Buresova, O. and Krivanek, J., *The Mechanisms and Applications of Leao's Spreading Depression of Electroencephalographic Activity*, Academic Press, NY, 1976.

5 Caspers, H., Speckmann, E.J. and Lehmenkühler, A., DC potentials of the cereòral cortex: seizure activity and changes in gas pressures, *Rev. Physiol. Biochem. Pharmachol.*, 106 (1987) 127–178.

6 Chesler, M. and Kraig, R.P., Intracellular pH transients of mammalian astrocytes, *J. Neurosci.*, 9 (1987) 159–174.

7 Cornel-Bell, A.H., Finkebeiner, S.M., Cooper, M.S., Smith, S.J., Glutamate induces calcium waves in cultured astrocytes: long range glial signalling, *Science*, 274 (1990) 470–473.

8 Deitmer, J.W. and Schlue, W.R., Intracellular Na and Ca in leech Retzius neurones during inhibition of the Na-K pump, *Pflügers Arch.*, 397 (1983) 195–201.

9 DoCarmo, R. and Martins-Ferreira, H., Spreading depression of Leao probed with ion-sensitive microelectrodes in isolated chicken retina, *Ann. Acad. Bras. Cienc.*, 56 (1984) 401–421.

10 Dowling, J.E., *The Retina. An Approachable Part of the Brain*, Harvard Univ. Press, Cambridge, MA, 1987.

11 Gardner-Medwin, A.R., A study of the mechanism by which potassium moves through brain tissue in the rat, *J. Physiol.*, 335 (1983): 353–374.

12 Gardner-Medwin, A.R. and Nicholson, C., Changes of extracellular potassium activity induced by electric current through brain tissue in the rat, *J. Physiol.*, 335 (1983) 375–392.

13 Gouras, P., Spreading depression of activity in amphibian retina, *Am. J. Physiol.*, 195 (1958) 28–32.

14 Hanke, W., Fernandes de Lima, V.M. and Schlue, W.R., Single ion channel behaviour measured in the intact chicken retina during spreading depression. In A. Lehmenkühler, K.H. Grotemeyer and F. Tegtmeyer (Eds.), *Migraine Basic Mechanisms and Treatment*, Urban-Schwarzenberg, Munich, in press.

15 Karwoski, C.J., Coles, J.A., Lu, H. and Huang, B., Current-evoked transcellular K flux in frog retina, *J. Neurophysiol.*, 61 (1989) 939–952.

16 Leao, A., Spreading depression of activity in the cerebral cortex, *J. Neurophysiol.*, 7 (1944) 359–390.

17 Lehmenkühler, A., Spreading depression-Reaktionen an der Hirnrinde: Störungen des extrazellularen Micromileus, *Z. EEG, EMG*, 21 (1990) 1–6.

18 Lehmenkühler, A., Speckmann, E.J. and Caspers, H., Cortical depression in relation to potassium activity, oxygen tension, local flow and carbon dioxide tension. In: M. Kessler, L.C. Clark, D.W. Lubbers, I.A. Silver and W. Simon (Eds.), *Ion and Enzyme Electrodes in Biology and Medicine*, Urban and Schwarzenberg, München, 1976.

19 Martins-Ferreira, H., Oliveira Castro, G., Struchiner, C.J. and Rodrigues, P.S., Circling spreading depression in isolated chick retina, *J. Neurophysiol.*, 37 (1974) 773–783.

20 Martins-Ferreira, H., Spreading depression in the chicken retina. In T. Ookawa (Ed.), *The Brain and Behaviour of the Fowl*, Jpn. Scient. Soc. Press, Tokio, 1983, 317–333.

21 Miller, R.F. and Dowling, J.E., Intracellular responses of the Müller (glia) cells of mudpuppy retina: their relation to b-wave of the eletroetinogram, *J. Neurophysiol.*, 33 (1970) 323–341.

22 Mody, I., Lambert, J.C.D. and Heinemann, U., Low extracellular magnesium induces epileptic activity and spreading depression in rat hippocampal slices, *J. Neurophysiol.*, 57 (1987) 869–888.

23 Mori, S., Miller, W.H. and Tomita, T., Microelectrode study of spreading depression (SD) in frog retina - general observations of field potentials associated with SD, *Jpn. J. Physiol.*, 26 (1976) 203–217.

24 Mori, S., Miller, W.H. and Tomita, T., Microelectrode study of spreading depression(SD) in frog retina - Müller cell activity and (K) during SD, *Jpn. J. Physiol.*, 26 (1976) 219–233.

25 Mori, S., Miller, W.H. and Tomita, T., Müller cell function function during spreading depression in frog retina, *Proc. Natl. Acad. Sci. USA*, 73 (1976) 1351–1354.

26 Newman, E.A., Electrophysiology of retinal glial cells, *Prog. Retinal Res.*, 8 (1989) 154–171.

27 Nicholson, C., Comparative neurophysiology of spreading depression in the cerebellum, *Ann. Acad. Bras. Cienc.*, 56 (1984) 481–494

28 Reichenbach, A., Dettmer, D., Reichelt, W. and Eberhardt, W., Na,K activated adenosine triphosphatase of isolated Müller cells from the rabbit shows a K dependence similar to that of the brain astrocytes, *Neurosci. Lett.*, 75 (1985) 281–284.

29 Reichenbach, A., Dettmer, D., Reichelt, W. and Eberhardt, W., High Na affinity of the Na,K pump in isolated rabbit retinal Müller (glial) cells, *Neurosci. Lett.*, 75 (1987) 157–162.

30 Schlue, W.R., Wuttke, W. and Deitmer, J.W., Ion activity measurements in extracellular spaces, nerve and glial cells in the central nervous system of the leech. In M. Kessler (Ed.), *Ion Measurements In Physiology and Medicine*, Springler, Berlin, 1985, pp. 166–173.

31 Schlue, W.R., Dörner, R., Rempe, L. and Riehl, B., Glial H transport and control of pH, *Ann. NY Acad. Sci.*, 633 (1991) 287–305.

32 Siesjo, B.K., Calcium in the brain under physiological and pathological conditions, *Eur. Neurol.*, 30 (suppl. 2) (1990) 3–9.

33 Somjen, G.G., Electrogenesis of sustained potentials, *Progr. Neurobiol.*, 1 (1973) 201–237.

34 Tomita, T., Spreading depression potential (SDP) in the frog retina, *Ann. Acad. Bras. Cienc.*, 56 (1984) 505–518.

35 Walz, W., Accumulation of intracellular bicarbonate accounts for the missing anion during potassium evoked swelling of cortical type-1 astrocytes, *Ann. NY Acad. Sci.*, 633 (1991) 589–591.